

Research on Optical Communication Transmission Characteristics Based on Nano - temperature Sensor and Its Application

Hua Zhao, Qing Lv*

Hebei Normal University, Hebei, China
 lvqingtougao@126.com

In this paper, a nano-scale surface plasmon structure type temperature sensor was proposed. Through the theoretical analysis and numerical simulation, the temperature sensing characteristics of the system were studied. The nano temperature sensor consists of a metal-medium-metal structure SPPs waveguide and an ethanol-sealed rectangular cavity. The effects of electromagnetic wave transmission, field intensity distribution, temperature sensing characteristics and structural parameters on temperature sensitivity and coupling strength were studied. It was found that the effective refractive index of SPPs decreased linearly with the increase of temperature in the subwavelength structure of silver-ethanol-silver. The transmission spectrum of the temperature sensor has two transmission peaks at 600nm~1800nm, and the peak wavelength has blue shift with the increase of temperature. Further analysis shows that the peak wavelength of the transmission has a linear relationship with the temperature, and the ambient temperature can be detected by detecting the change of the formant. The results show that the sensitivity of the nanometer temperature sensor is related to the length of the rectangular cavity and the thermal coefficient of the liquid sealed in the nanometer rectangular cavity. The structure can obtain the temperature sensing sensitivity of $-0.65\text{nm}/^{\circ}\text{C}$.

1. Introduction

Surface Plasmon Polaritons (SPPs) are electronically propagating electrons that propagate along the metal surface by electrons interacting with photons on the metal surface. Since the surface plasmon can overcome the diffraction limit of the light, the surface plasmon can realize the transmission, processing and related application of the optical signal at the nanometer scale (Wu et al., 2014). In recent years, with the progress of nano-processing technology, surface plasmon temperature sensor has been put out and gets the relevant theoretical research and experimental research (Poletti et al., 2013). The plasma resonance characteristics are sensitive to the dielectric properties of the surrounding environment and the shape of the metal microstructure. By fixing the incident light wavelength and scanning incidence angle, Sahin et al. track the variation of the resonance angle (the minimum value of the reflection intensity) with the outside temperature (Arwatz et al., 2015). In fact, these localized surface plasmon resonance (LSPRs) temperature sensors are relatively large in size, and they are all non-planar waveguides, so they are not easy to integrate with the chip. To meet the requirements of integration and compact structure, we present a novel SPPs temperature sensor. The sensor consists of a surface-plasma waveguide coupled with an ethanol-filled rectangular cavity. Two-dimensional finite difference time domain method (FDTD) and perfect matching layer (PML) boundary conditions are used to simulate and analyze the temperature sensing characteristics. We systematically analyze the relationship between SPPs transmission peak (formant) and ambient temperature. In addition, the effect of structural parameters on sensor sensitivity was analyzed to optimize the performance of the sensor. At present, there is no other research group to do SPPs waveguide temperature sensor system research (Yang et al., 2015). In our previous work, we proposed to use SPPs waveguide to do nano scale temperature sensor. We have a detailed system analysis of the SPPs waveguide designed as a temperature sensor for the first time. The research results will promote the application of SPPs waveguide.

2. Methods

In this paper, we propose the SPPs nanometer temperature sensor structure, which consists of two SPPs waveguide and a rectangular resonator. The rectangular nano-cavity is filled with ethanol, and the experiment can be filled with ethanol through the capillary attraction. Ethanol is sealed by other surfaces of the upper surface of the silver film in the rectangular cavity. The structure can be deposited on the substrate by a focused ion beam (Strata FIB201, FEI Company) or the silver film is deposited on the substrate. Light can be passed through the nanometer fiber into the sensor, and the output light can be measured by JY confocal Raman microscope. To reduce the computational memory and reduce the computational burden, we perform a two-dimensional finite-difference time-domain simulation in this paper. In the two-dimensional model, d is the slit width of the slit waveguide, w is the coupling distance between the slit waveguide and the rectangular cavity, and L and H are the length and height of the rectangular cavity, respectively.

In the metal-insulated dielectric-metal (MIM) waveguide, the dispersion relation of the fundamental mode of the TM wave can be written as (Kong, et al., 2016):

$$\varepsilon_d k_{z2} + \varepsilon_d k_{z1} \coth\left(-\frac{ik_{z1}}{2}d\right) = 0 \quad (1)$$

In the above formula, K_{z1} and K_{z2} are defined by momentum conservation as:

$$k_{z1}^2 = \varepsilon_d k_0^2 - \beta^2 \quad (2)$$

$$k_{z2}^2 = \varepsilon_m k_0^2 - \beta^2 \quad (3)$$

ε_d and ε_m are the dielectric constants of the electrolyte and the metal, respectively. β is the transmission constant of SPPs. The complex permittivity of silver is analyzed by Palik experimental data and interpolated by simulation (Rakhshani et al., 2016). The refractive index of ethanol is defined as:

$$n = 1.36048 - 3.94 \times 10^{-4}(T - T_0) \quad (4)$$

In the above formula, $T_0=20$ °C is room temperature. T is the ambient temperature. The thermal absorption of ethanol is high, and the thermal coefficient of silica is about $a=8.6 \times 10^{-6}$. The thermal coefficient of silver is about equal to 9.3×10^{-6} . Because the thermal coefficient of ethanol is higher than that of silver and silica, the effect of temperature changes on the refractive index of silver and silica is negligible when analyzing temperature sensing.

The width of the slit is $d=50\text{nm}$, $d=100\text{nm}$, $d=150\text{nm}$. The wavelength is $\lambda=600\text{nm}$, $\lambda=1000\text{nm}$, $\lambda=1550\text{nm}$. The relationship between the effective index of SPPs and the temperature of silver - ethanol - silver slit waveguide structure was analyzed. It is clear that the effective refractive index of SPPs decreases as the temperature increases. In the range of -100 °C to 60 °C, the effective refractive index is a linear function with respect to temperature. According to the time coupling mode theory, the transmission T_1 of the sensor can be expressed as (Virk et al., 2014).

$$T_1 = \frac{\Gamma^2}{(\Delta\omega)^2 + (\Gamma_0 + \Gamma)^2} \quad (5)$$

In the above formula, $\Delta\omega=\omega-\omega_0$, $\Gamma_0=1/\tau_0$, $\Gamma=1/\tau_-+1/\tau_+$, $1/\tau_0$ is the attenuation rate due to the intrinsic loss of SPPs. $1/\tau_-$ and $1/\tau_+$ are the coupling efficiency of the left SPPs waveguide and the cavity and the coupling efficiency of the cavity and the right SPPs waveguide, respectively. In our structure, $1/\tau_-=1/\tau_+$.

In this rectangular cavity, the cumulative phase shift of each SPPs is:

$$\Phi = 4\pi n_{\text{eff}} L / \lambda + 2\varphi \quad (6)$$

In the above formula, Φ is the phase shift of SPPs generated at the metal wall of the rectangular cavity, n_{eff} is the effective refractive index of SPPs, and L is the length of the rectangular cavity. At the resonant wavelength λ_0 , the incident light intensity can pass through the rectangular cavity and produce a peak at the transmission spectrum. The phase relationship at resonance is:

$$\Phi = 4\pi n_{eff} L / \lambda_0 + 2\varphi = 2m\pi \quad (7)$$

In the above formula, m is an integer. According to the Eq(7), the resonant wavelength can be written as:

$$\lambda_0 = 2n_{eff} L / (m - \varphi / \pi) \quad (8)$$

Only when the wavelength of the Eq(8) is satisfied, can it be transmitted efficiently in the structure. According to the Eq(8), the resonant wavelength λ_0 is proportional to the effective refractive index of SPPs. The effective refractive index is inversely proportional to the temperature, so the relationship between the resonant wavelength and the temperature can be obtained. The scale factor (temperature sensitivity) is:

$$\frac{d\lambda_0}{dT} = 2 \frac{dn_{eff}}{dT} L / (m - \varphi / \pi) \quad (9)$$

Due to the sensitivity of the nanostructures to changes in the refractive index of the dielectric material, the plasma waveguide and the ethanol sealed rectangular cavity coupling structure can be used to measure the temperature. As the temperature increases, the refractive index of the thermo-light effect ethanol is decreased, resulting in a change in the effective refractive index of the SPPs and a drift of the resonant wavelength. In order to investigate the temperature sensing properties of the structure, we use the FDTD method to establish the physical model. In the simulation, all external boundaries of the model take PML, and set the TM wave as the excitation source at the port on the left side of the slit. The grid size in the x and y directions is set to 5 nm x 5 nm. The time step can be made by Courant's condition:

$$\Delta t = \frac{0.95}{c} \sqrt{(\Delta x)^{-2} + (\Delta y)^{-2}} \quad (10)$$

In the above formula, C represents the speed of light in the vacuum. We set the two power monitors P1 and P2, respectively, to detect and record the excitation power (simulation removed from the resonant cavity involved in this chapter) and transmission power (with cavity structure). The distance between P1 and P2 is set to 1400 nm. The transmission of the sensor is defined as $T1 = P_{out} / P_{in}$. When the wavelength satisfies the identity (8), these wavelengths will get the maximum transmission.

3. Simulation and analysis

This paper presents a nanometer temperature sensor with SPPs waveguide and ethanol filled rectangular cavity coupled structure. The ability of the sensor to detect the temperature is attributed to the linear shift of the resonance wavelength caused by the thermal effect of ethanol. The sensitivity of the temperature sensor is related to the length and height of the resonator, and the thermo optic coefficient of the filled liquid. The results of two - dimensional FDTD simulation show that the temperature sensitivity of the nanometer sensor can reach 0.65nm /°C by selecting reasonable structural parameters. Its ultra-compact construction and planar waveguide structure is conducive to integration with the chip. In addition, the nano-device filter characteristics can be controlled by temperature, and it can be used as an adjustable SPPs filter. The simulation results obtained by us have some guiding significance for the design of nanoelectronic devices.

Figure 1 shows the transmission spectrum of the sensor at temperature $T=20$ °C. The width of the slit waveguide d is 50nm, the coupling distance w of the slit waveguide and the ethanol sealed rectangular cavity is 10nm, and the length L of the rectangular nanometer cavity and the height H are 450nm and 275nm respectively. It can be seen from Figure 1, at 600nm~1800nm, the structure of the transmission spectrum has two transmission peaks, which are marked as the peak A and peak B. The wavelengths corresponding to peaks A and B are resonant wavelengths of 1483.4 nm and 752.3 nm, respectively. The transmission of peak A is close to 19% and the transmission of peak B is about 45%. The transmission loss of the peak A is greater than the transmission loss of the peak B. In addition, the full of at half maximum (FWHM) of the peaks A and B is 55.6 nm and 31.1 nm, respectively.

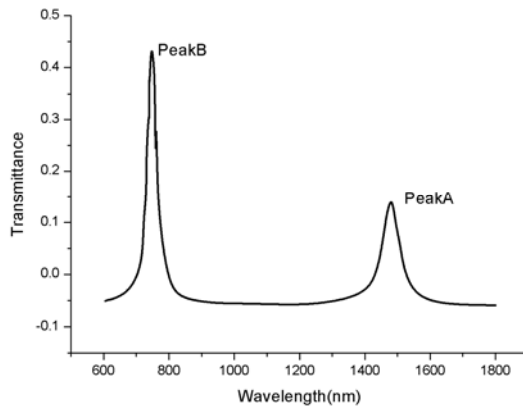


Figure 1: The distribution of field components HZ at different wavelengths

In the next step, we will study the temperature sensing properties of the nanodevice by investigating the effect of temperature on the transmission spectrum. The structural parameters are $d=50\text{nm}$, $w=10\text{nm}$, $L=450\text{nm}$, $H=275\text{nm}$, and the temperature rises from $-100\text{ }^{\circ}\text{C}$ to $60\text{ }^{\circ}\text{C}$. The simulated temperature step is $20\text{ }^{\circ}\text{C}$. Figure 2 (a) and Figure 2 (b) show the propagation spectra of peaks A and B with temperature. It can be seen from the figure that the transmission spectrum appears with the green shift phenomenon (drift to the short wave direction) as the temperature increases. According to the equations (2) and (8), it can be seen that the refractive index of ethanol decreases with the increase of temperature. The transmission peak wavelength (resonant wavelength) decreases with the decrease of the effective refractive index of SPPs in the nanometer cavity. The effective refractive index of SPPs decreases with the increase of temperature. It is easy to deduce that the resonance wavelength decreases as the temperature increases. Therefore, the FDTD simulation results are consistent with the theoretical analysis.

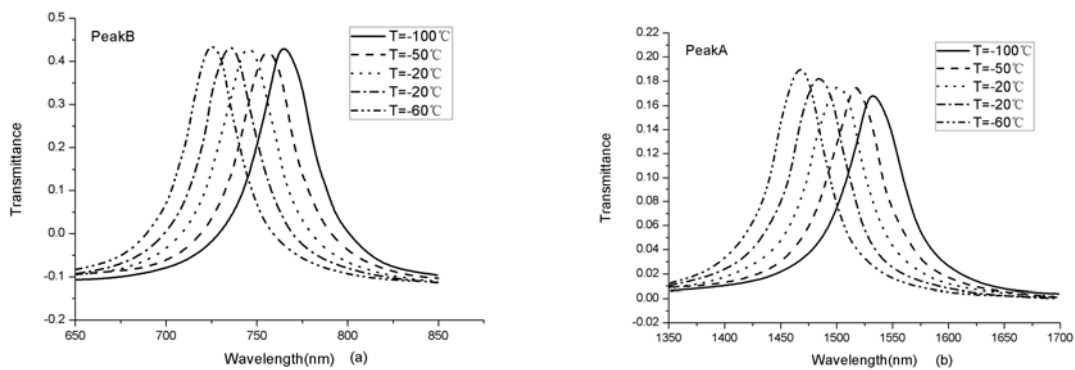


Figure 2: Two resonant wavelengths (peaks A and B) vary with temperature.

The structural parameters are $d=50\text{nm}$, $w=10\text{nm}$, $L=450\text{nm}$, $H=275\text{nm}$. It can be seen from the figure that the resonant wavelength is linearly related to the temperature. As the temperature increases, the resonant wavelength drifts to the shortwave direction. Obviously, by measuring several groups of resonant wavelength and temperature data, we can find their linear function expression, and then introduce any observed resonance wavelength into the function expression, we can get the corresponding ambient temperature. Figure 3 (b) shows the change in the resonant wavelength drift with temperature. The temperature rises from $100\text{ }^{\circ}\text{C}$ to $60\text{ }^{\circ}\text{C}$. The drift amount of the peak A is -68.20 nm and the drift amount of the peak B is -34.23 nm . The temperature sensitivity of peak A and peak B is $-0.43\text{ nm}/^{\circ}\text{C}$ and $-0.21\text{ nm}/^{\circ}\text{C}$, respectively, defined by temperature sensitivity $d\lambda/dT$. The temperature sensitivity of peak A is about 2 times of peak B. However, the disadvantage is that the loss of peak A is larger. The boiling points of ethanol were -114 and 78.4 DEG C ,

respectively. Because the sensor is only suitable for low temperature sensing, of course, we can fill the high boiling point of the liquid to do high temperature sensing.

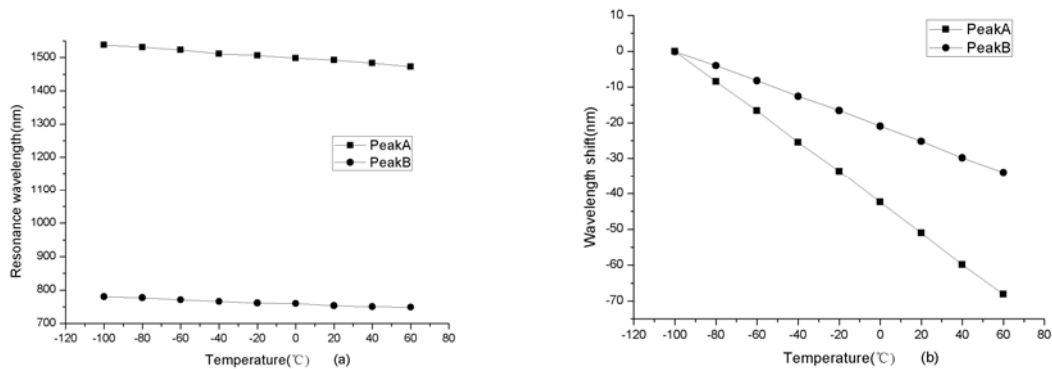


Figure 3: (a) The relationship between the resonant wavelength and the temperature of the sensor; (b) The relationship between resonance wavelength shift and temperature.

The temperature sensitivity of the peak A is much larger than that of the peak B. In practical applications, we prefer to detect the temperature of the peak A by detecting the drift of the peak A. Figure 4 (a) shows the change of the transmission peak A with the height of the rectangular cavity H. The temperature is constant at 20 °C, and other structural parameters are $d=50\text{nm}$, $w=10\text{nm}$, $L=450\text{nm}$. As can be seen from Figure 4 (a), the height is not more than 425nm. With the increase of the height of the rectangular cavity H, the transmission spectrum is shifted to short wave and the transmission loss is increased. Figure 4 (b) shows the effect of nano-rectangular cavity height on sensor sensitivity. The parameters are $d=50\text{nm}$, $w=10\text{nm}$. The rectangular cavity lengths are 360 nm, 450 nm, and 540 nm, respectively. The rectangular cavity height varies from 50 nm to 450 nm. When the height of the rectangular cavity is increased from 50nm to 80nm, the temperature sensitivity of peak A is decreased drastically. When the height of the rectangular cavity is increased from 80nm to 280nm, the temperature sensitivity of the peak A is reduced. When the height of the rectangular cavity exceeds 280nm, the temperature sensitivity of the peak A varies little with height, that is, the temperature of the rectangular cavity is very small. The results show that the decrease of the height of the rectangular cavity can not only improve the temperature sensitivity of the sensor, but also reduce the optical loss. Therefore, we increase the sensitivity of the sensor by increasing the length of the rectangular nano cavity or reducing the cavity height. When the slit width of the gap waveguide is 50nm, the coupling distance is 10nm, the length and width of the nano rectangular cavity are 540nm and 50nm respectively, and the temperature sensitivity of the peak A can be increased to $-0.65\text{nm}/^\circ\text{C}$.

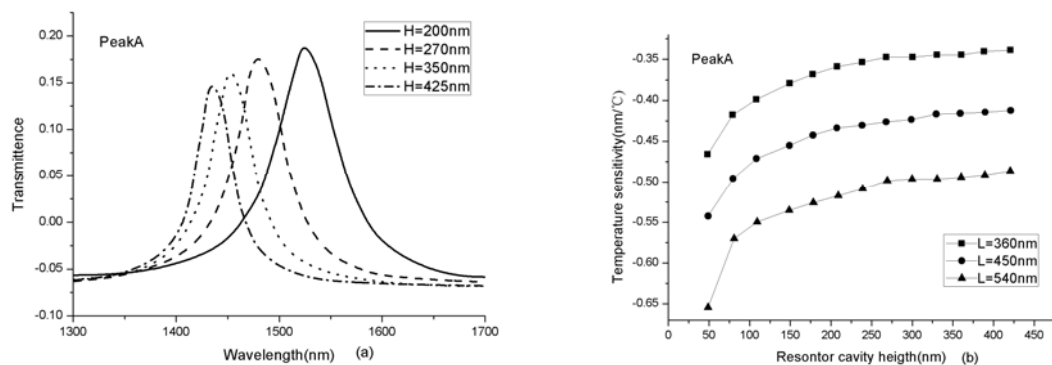


Figure 4: (a) The transmission peak A varies with the height of the nanometer rectangle; (b) The temperature sensitivity varies with the height of the nanometer rectangular cavity.

In addition, we can choose a higher thermal coefficient of liquid filled into the nano-rectangular cavity. In this way, we can get higher temperature sensitivity. As far as we know, the nano-SPPs temperature sensor temperature sensitivity is not much lower than the practical fiber temperature sensor. In practical applications, by considering the use of glycolic acid copolymer instead of ethanol, we can make all solid-state nano-devices. In addition, we propose a structure that can be used as a refractive index sensor or biosensor. The wavelength of the SPPs corresponding to the transmission peaks can be effectively transmitted in the structure, while the propagation of the other wavelengths in the structure is prohibited (Trung et al., 2016). Therefore, we propose a structure that can be used as a modulating filter for SPPs with temperature control.

4. Conclusions

A nano temperature sensor with SPPs waveguide and ethanol filled rectangular cavity coupled structure was proposed. The ability of the sensor to detect the temperature is attributed to the linear shift of the resonance wavelength caused by the thermal effect of ethanol. The sensitivity of the temperature sensor is related to the length and height of the resonator, and the thermo optic coefficient of the filled liquid. The results of two - dimensional FDTD simulation show that the temperature sensitivity of the nanometer sensor can reach 0.65nm/°C by selecting reasonable structural parameters. Its ultra-compact construction and planar waveguide structure is conducive to integration with the chip. In addition, the nano-device filter characteristics can be controlled by temperature, and it can be used as an adjustable SPPs filter. The simulation results have some guiding significance for the design of nanoelectronic devices.

Reference

- Arwatz G., Fan Y., Bahri C., Hultmark M., 2015, Development and characterization of a nano-scale temperature sensor (T-NSTAP) for turbulent temperature measurements, *Measurement Science and Technology*, 26(3), 035103, DOI: 10.1088/0957-0233/26/3/035103.
- Kong Y., Qiu P., Wei Q., Quan W., Wang S., Qian W., 2016, Refractive index and temperature nanosensor with plasmonic waveguide system, *Optics Communications*, 371, 132-137, DOI: 10.1016/j.optcom.2016.03.072.
- Poletti F., Wheeler N.V., Petrovich M.N., Baddela N., Fokoua E.N., Hayes J.R., Richardson D.J., 2013, Towards high-capacity fibre-optic communications at the speed of light in vacuum, *Nature Photonics*, 7(4), 279-284.
- Rakhshani M.R., Mansouri-Birjandi M.A., 2016, Utilizing the metallic nano-rods in hexagonal configuration to enhance sensitivity of the plasmonic racetrack resonator in sensing application, *Plasmonics*, 1-8, DOI: 10.1007/s11468-016-0351-x.
- Trung T.Q., Ramasundaram S., Hwang B.U., Lee N.E., 2016, An All - Elastomeric Transparent and Stretchable Temperature Sensor for Body - Attachable Wearable Electronics, *Advanced Materials*, 28(3), 502-509.
- Virk M., Xiong K., Svedendahl M., Käll M., Dahlin A.B., 2014, A thermal plasmonic sensor platform: resistive heating of nanohole arrays, *Nano letters*, 14(6), 3544-3549.
- Wu T., Liu Y., Yu Z., Peng Y., Shu C., He H., 2014, The sensing characteristics of plasmonic waveguide with a single defect, *Optics Communications*, 323, 44-48.
- Yang S.C., Hou J.L., Finn A., Kumar A., Ge Y., Fischer W.J., 2015, Synthesis of multifunctional plasmonic nanopillar array using soft thermal nanoimprint lithography for highly sensitive refractive index sensing, *Nanoscale*, 7(13), 5760-5766.